

## $\pi$ -Conjugated Ligand Polymers Entwined around Copper Centres

Pierre-Louis Vidal,<sup>[a]</sup> Bernadette Divisia-Blohorn,<sup>\*[a]</sup> Gérard Bidan,<sup>[a]</sup>  
Jean-Louis Hazemann,<sup>[b]</sup> Jean-Marc Kern,<sup>\*[c]</sup> and Jean-Pierre Sauvage<sup>[c]</sup>

**Abstract:** We describe conjugated polymers entwined around Cu<sup>I</sup> with alternating  $\alpha$ -quaterthienyl (poly[Cu(T<sub>2</sub>)<sub>2</sub>]) or 3',4',3''',4''''-tetrahexyl- $\alpha$ -sexythienyl (poly[Cu(T<sub>3</sub>)<sub>2</sub>]) moieties and 1,10-phenanthroline complexing sites. Our strategy is to synthesise the 2,9-bis(oligothienyl)-1,10-phenanthroline precursors, then to assemble these ligands by means of Cu<sup>I</sup> templating followed by electropolymerisation. Poly[Cu(T<sub>2</sub>)<sub>2</sub>] shows separate electroactivities for Cu redox centres and conjugated backbones, whereas the electroactivities overlap in the case of poly[Cu(T<sub>3</sub>)<sub>2</sub>]. An X-ray absorption study on these polymers in

their reduced state at the Cu-K edge identifies, in both cases, four nitrogen atoms as the closest copper(I) neighbours. For poly[Cu(T<sub>2</sub>)<sub>2</sub>], the Cu<sup>I</sup> environment is a distorted tetrahedron similar to a monomer model compound, but with a slightly higher number of steric constraints. The Cu<sup>I</sup> environment for poly[Cu(T<sub>3</sub>)<sub>2</sub>] is a less distorted tetrahedron with an unusually short Cu<sup>I</sup>-N average bond length. Cu<sup>I</sup> removal in

poly[Cu(T<sub>2</sub>)<sub>2</sub>] induces an irreversible collapse of the structure, whereas the reversibility of Cu<sup>I</sup> binding is almost perfect for poly[Cu(T<sub>3</sub>)<sub>2</sub>], as the hexyl chains prevent irreversible gliding of the wires after copper removal. Combined electrochemical and resistance measurements reveal that the Cu centres in poly[Cu(T<sub>2</sub>)<sub>2</sub>] play the role of mechanical support for the structure with no significant electronic interactions with the conjugated backbone, whereas in the case of poly[Cu(T<sub>3</sub>)<sub>2</sub>] copper centres contribute to the conductivity of the structure.

**Keywords:** conducting materials · conjugation · copper · EXAFS spectroscopy · polymers

### Introduction

Electropolymerisation of pyrroles or thiophenes with pendant functional groups (a metal ion binding site, a redox group or complexes of transition metals) has turned out to be a powerful tool for the coating of electrode surfaces.<sup>[1]</sup> A

polymeric matrix with the desired functionality is indeed obtained and such electrodes have been extensively studied for electrocatalysis,<sup>[2]</sup> or for their ability to sense alkali<sup>[3]</sup> and transition metal ions.<sup>[4,5]</sup> However, in these cases, functional groups have been isolated from the conjugated polymer by an alkyl spacer arm and this results in the additivity of functional group and polymer properties. For example, in the case of rigid tetrahedral bis(1,10-phenanthroline) metal complexes anchored within a poly(pyrrole) matrix by saturated linkages, the electrochemical response of the conjugated backbone is not strongly affected by removal or subsequent reincorporation of the copper(I) or other transition metal ions in the complexing cavities.<sup>[4b]</sup> Furthermore, conductivity measurements on these films using the four-probe technique reveal no contribution of the metal centres to the conductivity of the poly(pyrrole) matrix.<sup>[4a]</sup>

More recently, studies on conjugated polymers with transition metals directly connected to the backbone began to be reported.<sup>[6-16]</sup> In these studies, the classical properties of organic conjugated polymers (extended electronic transport) were mixed with those of transition metal complexes (catalytic properties, magnetism, redox properties or photoactivity) and this resulted in some new properties for the hybrid system that were not evident after a simple addition of those of the two individual systems (cooperativity effect). Indeed, metal centres have been shown to enhance photoconductivity,<sup>[7]</sup> photo-

[a] Dr. B. Divisia-Blohorn, Dr. G. Bidan, Dr. P.-L. Vidal  
Laboratoire d'Electrochimie Moléculaire  
UMR 5819 CEA/CNRS/Université J. Fourier  
Département de Recherche Fondamentale sur la Matière Condensée  
CEA Grenoble, 17 rue des Martyrs  
38054 Grenoble Cedex 9 (France)  
Fax: (+33)4-76-88-51-45  
E-mail: bidan@cea.fr

[b] Dr. J.-L. Hazemann  
Laboratoire de Cristallographie  
UPR 5031 CNRS, BP166  
38042 Grenoble Cedex 9 (France)  
Laboratoire de Géophysique Interne et Tectonophysique  
UMR 5559, UJF-CNRS, BP 53, 38041 Grenoble Cedex 9 (France)  
Fax: (+33)4-76-88-10-38  
E-mail: hazemann@labs.polycnrs-gre.fr

[c] Prof. J.-M. Kern, Dr. J.-P. Sauvage  
Laboratoire de Chimie Organo-Minérale  
UMR 7513, Institut Le Bel  
Université Louis Pasteur  
4 rue Blaise Pascal, 67000 Strasbourg Cedex (France)  
Fax: (+33)3-88-60-73-12  
E-mail: sauvage@chimie.u-strasbg.fr

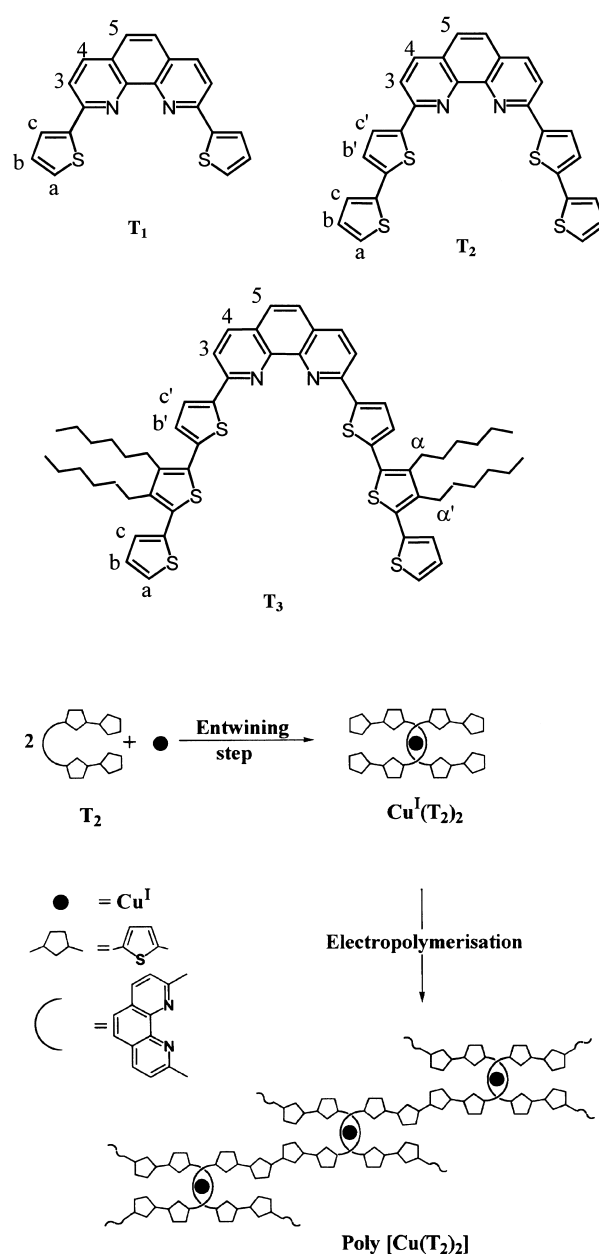
refractivity<sup>[13]</sup> or contribute in some cases to the conductivity of the conjugated structure.<sup>[9, 12]</sup> Moreover, electron density at a metal centre can be tuned by changing the redox state of the polymer backbone in the hybrid system described by Wrighton and Wolf;<sup>[8]</sup> such a polymer could potentially be used to modify the behaviour of a directly connected electrocatalytic group.

As a result of our interest in the study of electronic communication between metals and conducting polymers,<sup>[14, 16]</sup> we wish to report our own results from the synthesis and characterisation of conjugated ligand polymers entwined around copper ions with alternating 1,10-phenanthroline complexing units and oligothiophene wires. Our strategy is to synthesise 1,10-phenanthroline ligands with electropolymerisable oligothiophene of various lengths in positions 2 and 9 (ligands  $T_n$ , see structures), then to use  $\text{Cu}^I$  as a template<sup>[17]</sup> and this is followed by electropolymerisation of the  $[\text{Cu}(T_n)_2]^+$  complexes generated in the process. It is very important that the oligothiophene units are attached at the *ortho*-position of the 1,10-phenanthroline so as to strongly stabilise the copper centres.

Supramolecular architectures that consist of conjugated polymer wires, which have alternating oligothiophene moieties with well-defined lengths and phenanthroline complexing sites, entwined around copper centres are obtained as shown (poly $[\text{Cu}(T_n)_2]$ , Scheme 1).

A preliminary account of this study has been briefly reported;<sup>[18]</sup> the study showed that electropolymerisation of  $[\text{Cu}(T_2)_2]^+$  leads to the deposition of only a few layers, which do not contain copper, presumably due to steric hindrance around this metal as well as to the fact that the deposition potential required is too high. In this paper, we will show by

**Abstract in French:** *Un nouveau type de ligands polymères conjugués a été synthétisé. La stratégie mise en oeuvre est basée sur la synthèse des précurseurs électropolymérisables  $T_2$  et  $T_3$ , suivie de leur assemblage autour du  $\text{Cu}^I$ . Les complexes à ligands encastrés ainsi formés sont électropolymérisés, menant à des chaînes de polymères conjugués entrelacées autour du cuivre, alternant sites complexants 1,10-phénanthroline et  $\alpha$ -quaterthiophène (poly $[\text{Cu}(T_2)_2]$ ) ou 3',4',3''',4''''-tétrahexyl- $\alpha$ -sexithiophène (poly $[\text{Cu}(T_3)_2]$ ). Dans le cas de poly $[\text{Cu}(T_2)_2]$ , l'analyse par SAX au seuil K du cuivre montre un environnement autour de  $\text{Cu}^I$  analogue à celui des complexes de type  $[\text{Cu}^I(\text{dpp})_2]$  (i.e. géométrie tétraédrique distordue), bien que plus contraint stériquement. La présence de ce métal semble avoir peu d'influence sur le comportement électrochimique et sur la conductivité de la structure. En revanche, il joue un rôle de support mécanique essentiel: son enlèvement se traduit par un effondrement irréversible de la structure. Dans le cas de poly $[\text{Cu}(T_3)_2]$ , la SAX indique une géométrie du site de complexation de  $\text{Cu}^I$  de nature tétraédrique moins distordue, avec une distance moyenne  $\text{Cu}^I\text{-N}$  plus courte qu'à l'habitude. Les électroactivités respectives du squelette conjugué et du cuivre se recouvrent, et ce métal peut être exclu puis réincorporé de manière réversible, ce qui modifie à chaque fois profondément la réponse électrochimique de la structure. De plus, le métal apporte ici une contribution nette à la conductivité de poly $[\text{Cu}(T_3)_2]$ .*



Scheme 1. Schematic representation of the synthetic strategy (here for poly $[\text{Cu}(T_2)_2]$ ).

using cyclic voltammetry (CV) and X-ray absorption spectroscopy (XAS)<sup>[19]</sup> measurements that increasing the number of thiophene units leads to the desired poly $[\text{Cu}(T_2)_2]$  and poly $[\text{Cu}(T_3)_2]$  structures with quaterthiophene or alkylated sexithiophene moieties between copper bis(1,10-phenanthroline) complexes. Furthermore, XAS measurements reveal strong differences in terms of the  $\text{Cu}^I$  local environment between the two structures. The reversibility of  $\text{Cu}^I$  ion binding has also been studied in order to evaluate the interactions between metallic centres and the backbone; this was done by using CV and in situ resistance measurements for polymer films deposited on six-band microelectrode devices. From poly $[\text{Cu}(T_2)_2]$  to poly $[\text{Cu}(T_3)_2]$ , the reversibility of  $\text{Cu}^I$  ion binding and its contribution to the conductivity of the structure dramatically improve.

## Results and Discussion

**Synthesis and characterisation of the precursors  $T_n$  and of the corresponding entwined ligand complexes  $[\text{Cu}(T_n)_2]^+$ :** The synthetic procedure depicted in Scheme 2 is the same for all the ligands, that is, a necessary two-step nucleophilic addition to 1,10-phenanthroline, as previously described for the synthesis of the bithienyl-substituted ligand  $T_2$ , which is utilised for the formation of related conjugated poly(metallorotaxane) wires.<sup>[14, 16]</sup> The formation of the ligands was confirmed by 1D and 2D  $^1\text{H}$  NMR experiments, FABMS and elemental analysis.

$[\text{Cu}(T_n)_2]^+$  complexes are formed nearly quantitatively by reaction between  $T_n$  dissolved in  $\text{CH}_2\text{Cl}_2$  and  $[\text{Cu}(\text{CH}_3\text{CN})_4\text{BF}_4]$  in  $\text{CH}_3\text{CN}$  (2:1 stoichiometry). MS analysis and  $^1\text{H}$  NMR experiments confirm the formation of air- and light-stable complexes with the well-known entwined topography,<sup>[20]</sup> as confirmed by numerous shifts in  $^1\text{H}$  NMR signals induced by  $\text{Cu}^I$  templates.

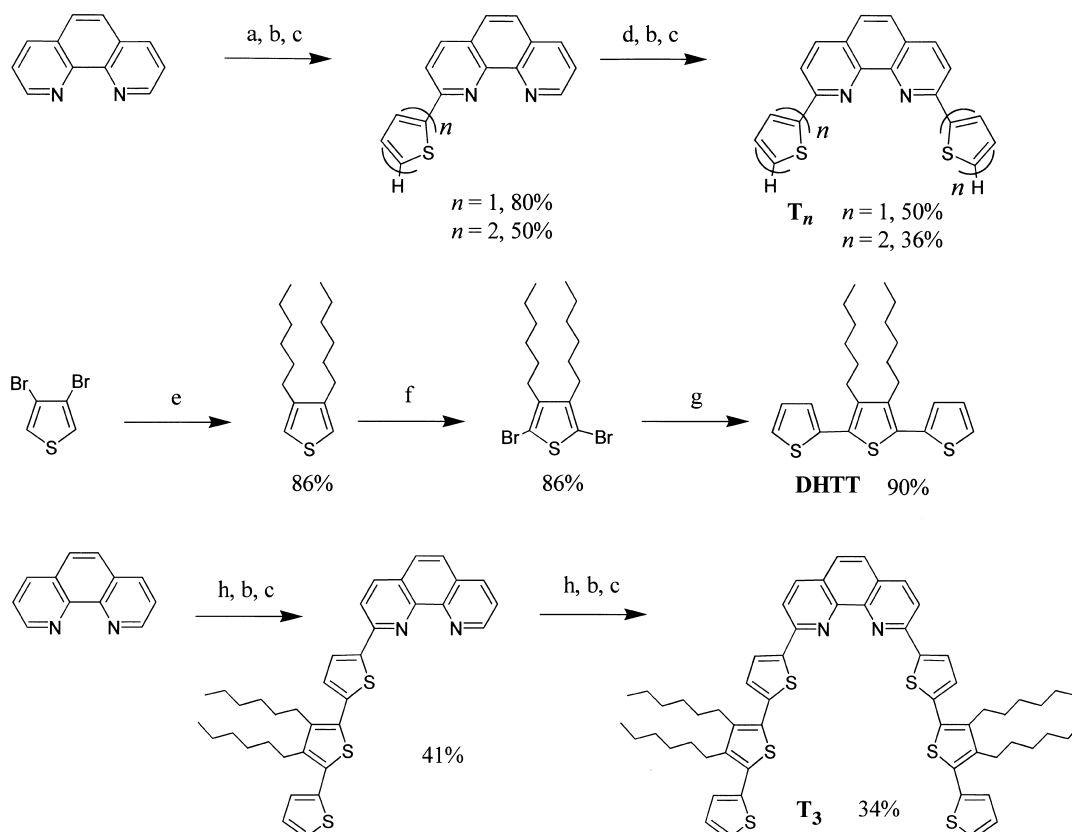
$[\text{Cu}(T_2)_2\text{BF}_4]$  has quite limited solubility in  $\text{CH}_3\text{CN}$  or  $\text{CH}_2\text{Cl}_2$ . On the assumption that the extension of the polymer with more thienyl units will reduce the solubility even further, two hexyl chains were introduced on the pendant electropolymerisable terthienyl units of the upper homologue ligand  $T_3$ . The compound 3',4'-dihexyl-2,2':5',2''-terthiophene (DHTT) was then preliminarily prepared according to a previously published synthetic procedure.<sup>[21]</sup> Because the two opposite

$\alpha$ -positions of DHTT are geometrically equivalent, no regio-selectivity problem could occur during nucleophilic addition on 1,10-phenanthroline derivatives (Scheme 2), and the hexyl groups on the central rings indeed induced good solubility in common organic solvents for  $T_3$  and  $[\text{Cu}(T_3)_2\text{BF}_4]$ .

A decrease in the yields of the two successive steps was observed from  $T_1$  to  $T_3$  (Scheme 2); this could be attributed to the increased inertness of the corresponding oligothiényllithium precursors. However, the difference between yields of  $T_2$  and  $T_3$  is low. We believe that the loss of reactivity due to the addition of one thienyl unit is, in this case, almost balanced by the donor effect induced by the hexyl chains.

UV/vis spectra of all the monomers and the corresponding  $\text{Cu}^I$  complexes have been recorded at room temperature in order to gain information on the electronic properties of these precursors. The main transitions are listed in Table 1. For the free ligands, a red shift is observed from  $T_1$  to  $T_3$ ; this is consistent with the extension of conjugation and with a broadening of the band in the 350–500 nm region caused by oligothiényl-based  $\pi \rightarrow \pi^*$  transitions. All the  $\text{Cu}^I$  complexes exhibit the well-known reasonably intense metal to ligand charge transfer (MLCT) bands<sup>[22]</sup> in the visible region; this is in agreement with the colour change observed upon addition of  $\text{Cu}^I$ .

**Electropolymerisation results:** All the polymers were synthesised by successive cyclic voltammetry (CV) on platinum



Scheme 2. The synthesis of the various precursor ligands. Reagents and conditions: a) for  $n=1$ , 2-thienyllithium, THF/toluene,  $0^\circ\text{C}$ ; for  $n=2$ , 2,2'-bithiophene, lithium diisopropylamide (LDA), THF/toluene,  $-78^\circ\text{C}$  then  $0^\circ\text{C}$ ; b)  $\text{H}_2\text{O}$ , room temperature; c) activated  $\text{MnO}_2$ ,  $\text{CH}_2\text{Cl}_2$ ; d) for  $n=1$ , 2-thienyllithium, THF,  $0^\circ\text{C}$ ; for  $n=2$ , 2,2'-bithiophene, LDA, THF,  $-78^\circ\text{C}$  then  $0^\circ\text{C}$ ; e)  $n$ -hexyl bromide, Mg,  $[\text{NiCl}_2(\text{dppf})]$  (2 mol %), THF, reflux; f)  $N$ -bromosuccinimide,  $\text{AcOH}/\text{CH}_2\text{Cl}_2$ ; g) 2-bromothiophene, Mg,  $[\text{PdCl}_2(\text{dppf})]$  (1 mol %),  $\text{Et}_2\text{O}$ , room temperature; h) DHTT, LDA, THF,  $-78^\circ\text{C}$  then  $0^\circ\text{C}$ .

Table 1. Colours and main UV/vis absorption transitions for the free ligands  $T_n$  and the related  $Cu^I$  complexes (sh = shoulder; spectra recorded with solutions ( $10^{-5}$  mol L $^{-1}$ ) in  $CH_2Cl_2$ ).

	colour	$\lambda_{max}$ [nm] [log $\epsilon$ ]
$T_1$	yellow	301[4.61], 330[4.32] 353[4.35], 372[4.23]
$T_2$	yellow/brown	345[4.74], 373[4.53] 390[4.57], 422(sh)[4.34]
$T_3$	red	365[4.73], 395[4.75] 440(sh)[4.48]
$[Cu(T_1)_2]^+$	red	340[4.86], 435[3.50] 490(sh)[3.36], 550(sh)[3.22]
$[Cu(T_2)_2]^+$	red/orange	335[4.72], 382[4.78] 540(sh)[3.36]
$[Cu(T_3)_2]^+$	dark red	318[4.70], 395[4.82] 467(sh)[4.54], 562(sh)[3.44]

or gold electrodes. All the potentials will be referenced versus the  $Ag/Ag^+$  ( $CH_3CN$ , 10 mmol L $^{-1}$ ) electrode.

As previously reported,<sup>[18]</sup> multisweep CV measurements on  $[Cu(T_1)_2BF_4]$  solutions (5 mmol L $^{-1}$ ) in  $CH_2Cl_2$  or  $CH_3CN$  led to the loss of copper ions and to the formation of only a few layers (a bleaching of the initially dark red  $[Cu(T_1)_2]^+$  solution was observed in the proximity of the working electrode during successive CV; this is indicative of decomplexation).

However, as expected, the addition of one thienyl unit allowed us to observe a simultaneous increase in the electroactivities of both the copper centres and the polymer matrix. This was carried out by successive CV between  $-0.2$  and  $1.25$  V of a  $[Cu(T_2)_2]^+$  solution (1 mmol L $^{-1}$ ) in  $CH_2Cl_2/Bu_4NPF_6$  (0.3 mol L $^{-1}$ ). The resulting poly $[Cu(T_2)_2]$  stable films are red in their reduced form and CV measurements in a monomer-free solution (Figure 1 top) display a reversible wave at  $0.68$  V, which corresponds to the copper redox process, as can be observed from the unchanged potential value relative to the monomer. The broad and reversible response between  $0.8$  and  $1.25$  V is very similar to that observed by cycling a poly $T_2$ <sup>[23]</sup> film in the same supporting electrolyte and thus has been attributed to the quaterthienyl moieties, which result from anodic coupling of monomers.

The ratio of metallic centres to backbone electroactivities is approximately 1:2.4 (determined by evaluation of charge quantities, which correspond to the metallic and the oligothieryl redox system, respectively). In other studies of related poly(metallorotaxane) wires using  $T_2$  as an electropolymerisable precursor,<sup>[14, 16]</sup> we have found that this ratio was 1:1.25. A result of 1:2.5 was thus expected in the present case for a perfect polymerisation: the ratio obtained thus confirms the nearly quantitative incorporation of the  $Cu^I$  ion used as crosslinking nodes in the conjugated structure.

From  $T_2$  to  $T_3$ , there is a loss of reactivity towards electropolymerisation, presumably due to the increased stability of the radical cations involved in the polymerisation mechanism<sup>[24]</sup> and to a higher solubility in the electrolytic medium of the alkylated oligomer species generated by anodic coupling. Indeed, successive cycling of a  $T_3$  solution (5 mmol L $^{-1}$ ) in  $CH_2Cl_2/Bu_4NPF_6$  (0.3 mol L $^{-1}$ ) between  $-0.1$  and  $0.75$  V led only to the deposition of a very thin dark red film. Cycling this deposit in a monomer-free solution in

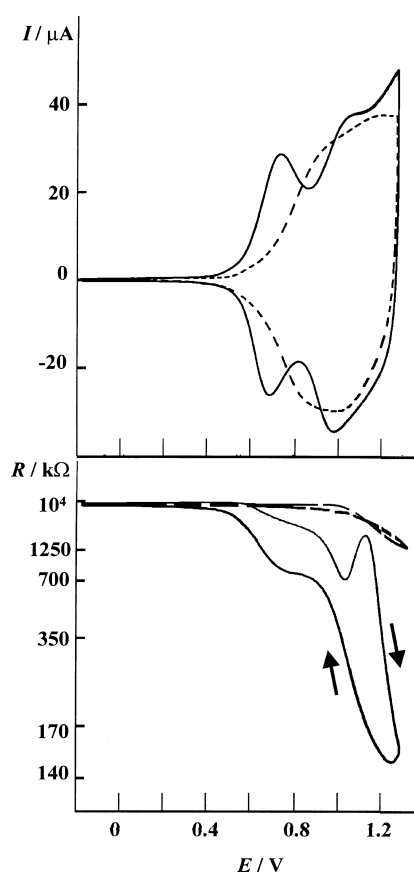


Figure 1. Top: Cyclic voltammetry in  $CH_2Cl_2/Bu_4NPF_6$  (0.3 mol L $^{-1}$ ) ( $v = 50$  mV s $^{-1}$ ) of a) a freshly prepared poly $[Cu(T_2)_2]$  film (solid line) and b) after dipping for 20 min in a  $Bu_4NCN$  solution (0.1 mol L $^{-1}$ ) in  $CH_3CN$  (dashed line). Bottom: related resistance measurements in  $Bu_4NPF_6$  (0.3 mol L $^{-1}$ ) in  $CH_2Cl_2$  ( $v = 2$  mV s $^{-1}$ ). Working electrode: six-band gold microelectrodes (5  $\mu m$  spacing).

$CH_2Cl_2$  resulted in its instantaneous solubilisation in the electrolytic medium. However, we reasoned that  $CH_3CN$  would be a less solubilising solvent and accordingly a black and thick deposit was indeed obtained by cycling a  $T_3$  solution (5 mmol L $^{-1}$ ) in  $CH_3CN/Bu_4NPF_6$  (0.1 mol L $^{-1}$ ) between 0 and 0.80 V. This film exhibits a very stable and broad electroactivity between 0.5 and 0.80 V in a monomer-free solution in  $CH_3CN$  (Figure 2A). The linear relationship between peak current intensity and sweep rate (10–100 mV s $^{-1}$ ) is indicative of the deposition of an electroactive polymer. Furthermore, the important cathodic shift (100 mV) of the oxidation process compared with poly $T_2$  is consistent with the immobilisation of an alkylated sexithienyl electroactive species.

Contrary to what is observed with the free ligand,  $[Cu(T_3)_2BF_4]$  solution (1.5 mmol L $^{-1}$ ) in  $CH_2Cl_2/Bu_4NPF_6$  (0.3 mol L $^{-1}$ ) readily electropolymerises (Figure 3) by continuous cycling between  $-0.1$  and  $0.97$  V.

The films generated are red in their reduced state. They exhibit a very stable electrochemical response in a monomer-free solution with two reversible waves centred at 0.6 and 0.75 V (Figure 4 top) and there are no further redox processes at potentials higher than 1 V. Since alkylated sexithiophenes are known to produce both radical cations and dication upon oxidation,<sup>[25–27]</sup> the roughly equal electroactivities of the two

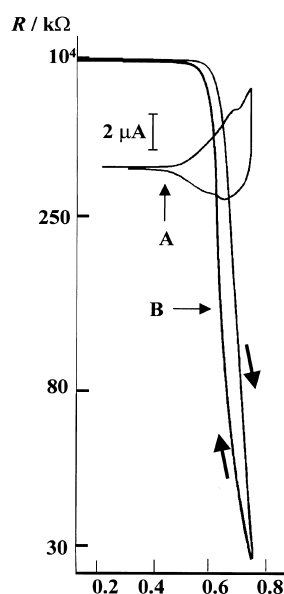


Figure 2. Cyclic voltammogram (A) and resistance measurements (B) in  $\text{CH}_3\text{CN}/\text{Bu}_4\text{NPF}_6$  ( $0.1 \text{ mol L}^{-1}$ ) ( $\nu = 2 \text{ mV s}^{-1}$ ) on a freshly prepared poly[ $\text{T}_3$ ] film using six-band platinum microelectrodes ( $2 \mu\text{m}$  spacing).

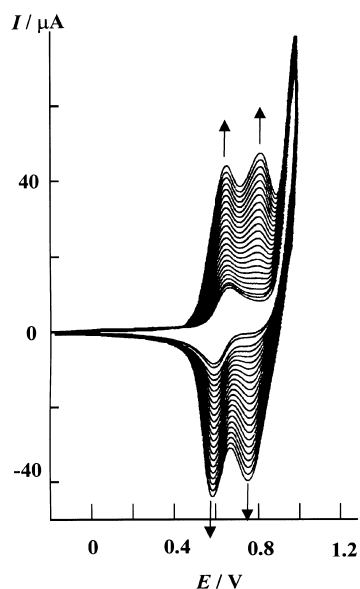


Figure 3. Cyclic voltammograms were recorded at  $100 \text{ mV s}^{-1}$  for the electropolymerisation of a  $[\text{Cu}(\text{T}_3)_2]^+$  solution ( $1.5 \text{ mmol L}^{-1}$ ) in  $\text{CH}_2\text{Cl}_2/\text{Bu}_4\text{NPF}_6$  ( $0.3 \text{ mol L}^{-1}$ ). The set of successive CV corresponds to a synthetic charge of  $50 \text{ mC cm}^{-2}$ .

successive waves (Figure 4 top) suggest that none of them could be assigned in its totality to the copper redox system and that there is a mixing of the copper and conjugated backbone redox processes. XAS spectroscopy at the Cu-K edge and demetallation/remetallation experiments described in the next two parts of this section will provide a conclusive answer to the question about the presence of copper in the conjugated structure and of the localisation of the redox processes.

**XAS spectroscopic studies on poly[ $\text{Cu}(\text{T}_2)_2$ ] and poly[ $\text{Cu}(\text{T}_3)_2$ ]:** Given that copper redox waves for poly[ $\text{Cu}(\text{T}_3)_2$ ] could not be detected precisely by cyclic voltammetry, XAS

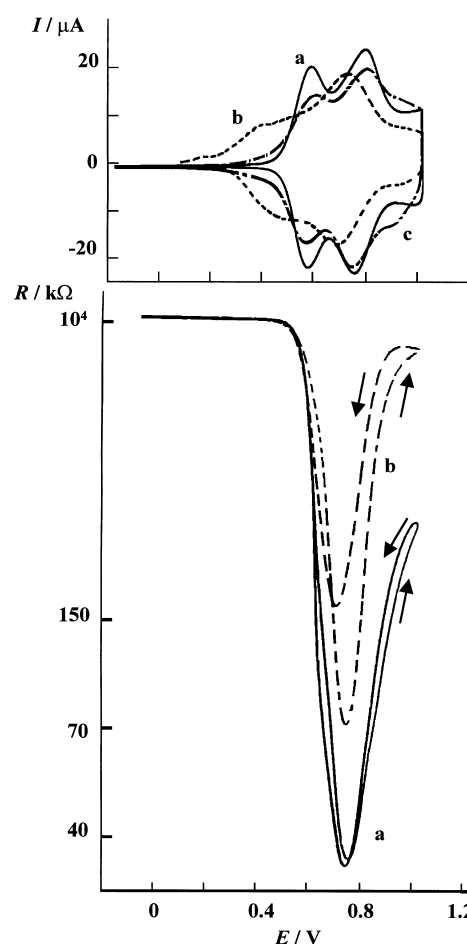


Figure 4. Top: cyclic voltammogram in  $\text{CH}_2\text{Cl}_2/\text{Bu}_4\text{NPF}_6$  ( $0.3 \text{ mol L}^{-1}$ ) ( $\nu = 50 \text{ mV s}^{-1}$ ) of a) a freshly prepared poly[ $\text{Cu}(\text{T}_3)_2$ ] film (solid line), b) after dipping for 20 min in  $\text{CH}_3\text{CN}/\text{Bu}_4\text{NCN}$  ( $0.1 \text{ mol L}^{-1}$ ) (dashed line) and c) after dipping for one hour in a  $[\text{Cu}(\text{CH}_3\text{CN})_2\text{BF}_4]$  solution ( $0.1 \text{ mol L}^{-1}$ ) in  $\text{CH}_3\text{CN}$  (dot and dashed line). Bottom: in situ resistance measurements in  $\text{CH}_2\text{Cl}_2/\text{Bu}_4\text{NPF}_6$  ( $0.3 \text{ mol L}^{-1}$ ) ( $\nu = 2 \text{ mV s}^{-1}$ ) using six-band gold microelectrodes ( $2 \mu\text{m}$  spacing) on a) a freshly prepared poly[ $\text{Cu}(\text{T}_3)_2$ ] film (solid line) and measurements b) after dipping for 20 min in  $\text{CH}_3\text{CN}/\text{Bu}_4\text{NCN}$  ( $0.1 \text{ mol L}^{-1}$ ) (dashed line).

studies at the Cu-K edge were expected to be particularly useful to assign the presence of the  $\text{Cu}^I$  template in this conjugated polymer. Furthermore, it was hoped that a comparative study of  $\text{Cu}^I$  binding sites between poly[ $\text{Cu}(\text{T}_2)_2$ ] and poly[ $\text{Cu}(\text{T}_3)_2$ ] would allow us to determine the influence of variation in the oligothieryl wire in terms of electronic and steric effects, since XAS spectroscopy represents a highly sensitive tool for the quantitative investigation of atomic and molecular details of noncrystalline materials such as electrochemical interfaces.<sup>[28]</sup>

An X-ray absorption study at the Cu-K edge on poly[ $\text{Cu}(\text{T}_2)_2$ ] and poly[ $\text{Cu}(\text{T}_3)_2$ ] in their reduced stable state was thus undertaken. The same monomer for the XAS study on a related poly(metallorotaxane) structure<sup>[16]</sup> was selected here as a reference compound, that is,  $[\text{Cu}^I(\text{dap})_2\text{BF}_4]$  [dap = 2,9-di(*p*-anisyl)-1,10-phenanthroline]. This was so that the chemical environment was as close as possible to the one envisaged for the polymers.<sup>[29]</sup> Furthermore, crystal structures of this compound<sup>[30]</sup> or of the related dpp complex<sup>[31]</sup> [dpp = 2,9-

diphenyl-1,10-phenanthroline] have been reported: the coordination geometry for the copper(I) centre in  $[\text{Cu}^{\text{I}}(\text{dap})_2]$  (Cu–N bond lengths: 2.053 and 2.067 Å) or  $[\text{Cu}^{\text{I}}(\text{dpp})_2]$  (Cu–N bond lengths: 2.019 and 2.112 Å for one dpp, 2.032 and 2.082 Å for the other) is best described as distorted and disymmetrical tetrahedral. XAS spectra of  $[\text{Cu}^{\text{I}}(\text{dap})_2\text{BF}_4]$  reference solutions have been recorded and analysed<sup>[16]</sup> and we present here a comparative analysis of the spectra recorded for the conjugated polymer samples in their reduced state.

**X-ray absorption near-edge (XANES) study:** The XANES measurements are very sensitive to the electronic structure and to the geometry around the copper ion.<sup>[32, 33]</sup> This region corresponds to  $1s \rightarrow 3d$  and  $1s \rightarrow 4p$  transitions of the excited photoelectron to vacant orbitals with p symmetry and the ordering of those vacant orbitals is dependent on the geometry of the copper coordination sphere. Therefore, a qualitative comparative XANES study between monomer and polymer spectra has been undertaken before X-ray absorption fine structure (EXAFS) analysis to gain structural information from the polymeric samples (Figure 5). First of all, none of the polymer spectra exhibit a pre-peak

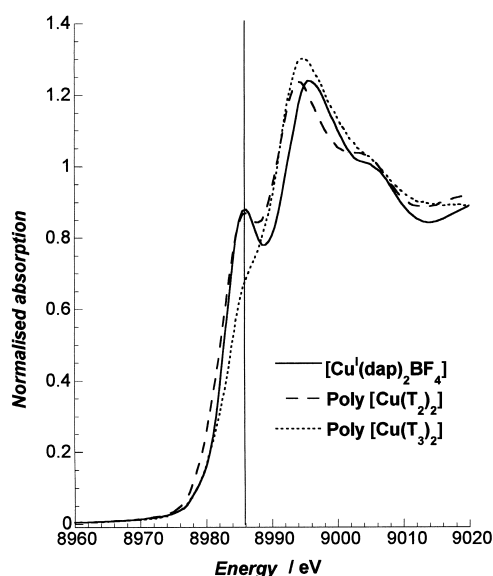


Figure 5. XANES spectra of the monomer model compound  $[\text{Cu}^{\text{I}}(\text{dap})_2\text{BF}_4]$  and of the poly $[\text{Cu}(\text{T}_n)_2]$  samples.

between 8975 and 8980 eV that corresponds to the  $1s \rightarrow 3d$  transition in the near-edge region; this is consistent with a  $\text{Cu}^{\text{I}} 3d^{10}$  species. Further evidence of a +1 redox state is provided by the absence of a significant shift of the edge towards higher energy, observed from the  $\text{Cu}^{\text{I}}$  to  $\text{Cu}^{\text{II}}$  species.<sup>[32, 33]</sup>

The XANES spectrum of  $[\text{Cu}^{\text{I}}(\text{dap})_2\text{BF}_4]$  mainly displays a strong first transition (pre-peak transition) at 8986 eV followed by the “white line” at 8996 eV. These two successive transitions result from a distortion of the tetrahedral environment;<sup>[30, 31]</sup> this leads to a splitting of the  $4p_{(x,y,z)}$  orbitals and thus they have been assigned to  $1s \rightarrow 4p_{x,y}$  and  $1s \rightarrow 4p_z$  transitions, which are typical of a  $\text{Cu}^{\text{I}}$  response in a distorted tetrahedral environment.<sup>[32, 33]</sup>

The poly $[\text{Cu}(\text{T}_2)_2]$  spectrum displays the same shape as that for  $[\text{Cu}^{\text{I}}(\text{dap})_2\text{BF}_4]$  without any significant edge shift: the intensity for the pre-peak transition and for the “white line” are identical for the two spectra (Figure 5). This suggests that the electronic structure and the topography of the  $\text{Cu}^{\text{I}}$  binding site are very similar in both cases.

In contrast, the shape of the poly $[\text{Cu}(\text{T}_3)_2]$  spectrum is very different to the previous ones: the pre-peak transition intensity, in this case, has strongly decreased, whereas the “white line” intensity is slightly higher. This is indicative of the weaker splitting of the  $4p_{(x,y,z)}$  orbitals and, unusually, of a less distorted tetrahedral environment for  $\text{Cu}^{\text{I}}$  in poly $[\text{Cu}(\text{T}_3)_2]$ . This could be ascribed to the quite bulky hexyl chains, which force the binding site to adopt this less distorted geometry to minimise the steric repulsion between two adjacent alkylated sexithiophenes. However, a study of related structures, which differ from poly $[\text{Cu}(\text{T}_3)_2]$  as a result of the alkyl chain length, would be necessary to check the validity of this assumption.

**EXAFS study:** Structural parameters have been extracted from EXAFS oscillations using the same procedure as for the related poly(metallorotaxane).<sup>[16]</sup> The structural parameters deduced from analysis of the spectra are summarised in Table 2 and the measurements for the Fourier filtered first shell of polymers poly $[\text{Cu}(\text{T}_2)_2]$  and poly $[\text{Cu}(\text{T}_3)_2]$  are presented in Figure 6.

In all cases, EXAFS identifies four nitrogen atoms as the closest neighbours. It is worth noting that all attempts to include one additional boron or nitrogen atom do not improve the fit or even lead to a worse one. The results of modelling

Table 2. Structural parameters for the fits of the different samples (values in parentheses are estimated uncertainties in the last digit).

modélisation	$R_1$ [Å]	$\sigma_1^2$ [ $10^3 \text{ \AA}^2$ ]	$R_2$ [Å]	$\sigma_2^2$ [ $10^3 \text{ \AA}^2$ ]
$[\text{Cu}(\text{dap})_2\text{BF}_4]^{\text{[a]}}$				
4N	2.03 (0.7)	7.1 (5)		
poly $[\text{Cu}(\text{T}_2)_2]^{\text{[a]}}$				
4N	2.04 (0.6)	9.2 (10)		
2N2N	1.97 (0.7)	2.5 (10)	2.12 (0.7)	1.6 (10)
poly $[\text{Cu}(\text{T}_3)_2]^{\text{[a]}}$				
4N	2.00 (0.4)	6.9 (6)		

[a]  $\Delta E^{\circ}$  held fixed at  $-1.8$  in accordance with edge shifts relative to reference spectrum  $[\text{Cu}^{\text{II}}(\text{dap})_2(\text{BF}_4)_2]$ [16].

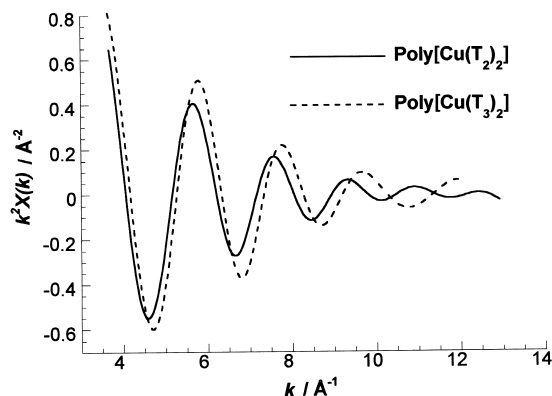


Figure 6. Fourier filtered first shell of the polymeric samples poly $[\text{Cu}(\text{T}_n)_2]$ .

with a single shell of four nitrogen neighbours (4N modelling) are in accordance with XANES analysis: for poly[Cu(T<sub>2</sub>)<sub>2</sub>], a first approach gave an average Cu<sup>I</sup>–N bond length of 2.04 Å.

loss of resolution of the electrochemical response of the oligothieryl moieties observed when  $\text{Cu}^{\text{I}}$  was removed (Figure 4b top) suggest strong electronic interactions between the copper centres and the conjugated backbone.

**In situ resistance experiments:** In order to evaluate quantitatively the interactions between the copper centres and the conjugated backbone, in situ cyclic voltammetry and relative resistance measurements have been performed. The principle of these measurements was inspired from the methodology developed years ago by Wrighton et al.<sup>[35]</sup> Gold and platinum microelectrode arrays with interelectrode spacing from 2 to 10  $\mu\text{m}$  have been used. Electrochemical deposition of the polymers allowed electrical connection of adjacent microelectrodes. The middle electrodes were the working electrodes of a classical three-electrode device connected to a Princeton Applied Research (PAR) device, whereas the two outside ones were connected to a stabilised power device. The resistance of the polymers was then recorded as a function of the applied potential. The sample depth was then measured for dried polymers in their reduced state with a profilometer; this allowed a good estimation of the in situ conductivity of the sample. Poly $\text{T}_2$ , poly $\text{T}_3$  and then freshly prepared and demetallated poly $[\text{Cu}(\text{T}_2)_2]$  and poly $[\text{Cu}(\text{T}_3)_2]$  structures have been investigated.

The resistance profile of poly $\text{T}_2$  (not shown) corresponds to the oxidation of the polymer. The signal, which does not evolve after exhaustive cycling, is similar to that of the previously reported *para*-bipyridyl-quaterthiophene copolymer.<sup>[12]</sup> In our case, the maximum of p-type conductivity has been evaluated to be  $1.2 \times 10^{-4} \text{ S cm}^{-1}$  at 1.15 V and is lower than the  $2 \times 10^{-3} \text{ S cm}^{-1}$  value reported for the analogous bipyridyl-based polymer. Presumably, the explanation is due to a higher delocalisation in a linear 5,5'-disubstituted 2,2'-bipyridine than in the U-shaped phenanthroline-based polymers described here.

The first scan of a freshly prepared poly $[\text{Cu}(\text{T}_2)_2]$  film gave the resistance profile depicted in Figure 1 (bottom), with a first drop (700 k $\Omega$ ) at 1.0 V, followed by a second more important one (150 k $\Omega$ ) at 1.2 V and a large hysteresis loop on the reverse scan. The resulting estimated conductivities are  $1.8 \times 10^{-5}$  and  $1.1 \times 10^{-4} \text{ S cm}^{-1}$ , respectively. Since this last value is very similar to that obtained with poly $\text{T}_2$ , the preforming of coordination sites by entwining ligands around  $\text{Cu}^{\text{I}}$  clearly has no influence on the conductivity of the structure. Further scans showed a strong evolution of the signal without any change in CV settings. The first drop completely disappeared after the first scan, whereas the second remained stable. Thus, the shape is very similar to that obtained for poly $\text{T}_2$  with no measurable contribution of the  $\text{Cu}^{\text{I}}/\text{Cu}^{\text{II}}$  oxidation process to the conductivity. This demonstrates the absence of significant electronic interactions between the copper centres and the conjugated backbone.

After the removal of  $\text{Cu}^{\text{I}}$  centres using cyanide as a complexing agent for the metal, an irreversible drop in the conductivity occurred (Figure 1 bottom). After two scans, the maximum dramatically fell to less than  $10^{-5} \text{ S cm}^{-1}$  with only a slight loss of electroactivity. Since  $\text{Cu}^{\text{I}}$  removal induces the

irreversible collapse of the structure (Scheme 3), the inter-chain interactions of the intertwined wires are probably destroyed.

The resistance profile of poly $\text{T}_3$  is depicted in Figure 2B and corresponds roughly to the oxidation of the polymer. The maximum for the p-type conductivity is at  $1 \times 10^{-4} \text{ S cm}^{-1}$  at 0.75 V; this value is of the same order as the highest value recorded for poly $\text{T}_2$ .

The case of poly $[\text{Cu}(\text{T}_3)_2]$  clearly contrasts with that of poly $\text{T}_3$ : a single and stable window of conductivity, which corresponds exactly to the oxidation of the polymer, was observed (Figure 4 bottom). The resistance drops approximately at the potential of the second redox wave with an estimated conductivity of  $9 \times 10^{-4} \text{ S cm}^{-1}$ , that is, one order of magnitude higher than that for poly $\text{T}_3$ . Furthermore, the profile of a demetallated film showed a decrease in this maximum ( $3 \times 10^{-4} \text{ S cm}^{-1}$ ) combined with a slight narrowing of the window of conductivity and the appearance of a hysteresis loop. Since we have proved in the previous section that, in the case of poly $[\text{Cu}(\text{T}_3)_2]$ , the architecture was completely preserved after  $\text{Cu}^{\text{I}}$  removal, this last result clearly shows that copper centres contribute to the conductivity of this structure.

## Conclusion

In conclusion, a new type of conjugated ligand polymer entwined around copper(I) has been synthesised. The strategy was based on the synthesis of 2,9-bis(oligothieryl)-1,10-phenanthroline precursors, followed by assembly of these ligands by means of  $\text{Cu}^{\text{I}}$  templates. The grafting of the oligothieryl units on the *ortho*-position of the 1,10-phenanthroline results in a strong stabilisation of copper ions. Subsequent electropolymerisation afforded conjugated polymers entwined around copper centres with alternating  $\alpha$ -quaterthieryl (poly $[\text{Cu}(\text{T}_2)_2]$ ) or 3',4',3''',4''''-tetrahexyl- $\alpha$ -sextiethieryl (poly $[\text{Cu}(\text{T}_3)_2]$ ) moieties and 1,10-phenanthroline complexing sites.

In the case of poly $[\text{Cu}(\text{T}_2)_2]$ , a XAS study has shown that the environment of copper is not substantially different (that is, in the form of a distorted tetrahedron) from that in the monomer model compound, but in poly $[\text{Cu}(\text{T}_2)_2]$  it has slightly higher steric constraints. Demetallation/remetallation experiments combined with in situ resistance measurements have shown that  $\text{Cu}^{\text{I}}$  plays the role of an essential mechanical support for the conjugated supramolecular structure, but it has no further significant electronic interactions with the conjugated ligand polymer.

In the case of poly $[\text{Cu}(\text{T}_3)_2]$ , there is less difference between the copper and backbone redox processes. XAS studies have shown that, for this compound, the  $\text{Cu}^{\text{I}}$  bonding takes the form of a slightly distorted tetrahedron with an unusually short average  $\text{Cu}^{\text{I}}\text{-N}$  bond length. The reversibility of  $\text{Cu}^{\text{I}}$  binding is perfect and removal of this ion results in a strong modification of the conjugated-backbone electrochemical response. Furthermore, in situ resistance measurements show that copper centres contribute to the conductivity of this conjugated structure.



## Experimental Section

**Reagents, chemical and electrochemical procedures:** Air- and moisture-sensitive reactions were carried out in oven-dried glassware under an argon atmosphere. CH<sub>3</sub>CN and toluene were distilled from CaH<sub>2</sub>. THF and ether were distilled from sodium benzophenone immediately before use. CH<sub>2</sub>Cl<sub>2</sub> used for electrochemical experiments was distilled from P<sub>2</sub>O<sub>5</sub> and stored in a dry box under an argon atmosphere. [Cu(CH<sub>3</sub>CN)<sub>4</sub>BF<sub>4</sub>] was prepared as previously described.<sup>[29]</sup> *n*Bu<sub>4</sub>NPF<sub>6</sub> was dried at 100 °C under vacuum and stored in a desiccator and all other commercially available reagents were used as received. <sup>1</sup>H NMR spectra were recorded with a AC200 Bruker or a U 400 Varian spectrometer. UV/vis absorption spectra were obtained using a Kontron Uvikon 860 spectrophotometer. Mass spectral analyses were performed by the Institut de Biologie Structurale, Grenoble (France). Elemental analyses were performed by the Département d'analyses élémentaires, CNRS, Solaize (France). Electrochemical synthesis and studies were performed under an argon atmosphere using a PAR273A from EG&G Princeton Applied Research and with a typical three-electrodes cell. The electrolyte solutions used were *n*Bu<sub>4</sub>NPF<sub>6</sub> (all 0.3 mol L<sup>-1</sup>) in CH<sub>2</sub>Cl<sub>2</sub>, except for the electro-synthesis and characterisation of polyT<sub>3</sub>, performed in a *n*Bu<sub>4</sub>NPF<sub>6</sub> solution (0.1 mol L<sup>-1</sup>) in CH<sub>3</sub>CN. All the potentials were relative to a Ag<sup>+</sup>/Ag reference electrode (10 mmol L<sup>-1</sup>) and were corrected such that *E*<sub>1/2</sub>(ferrocene) = 0.18 V, that is, the value obtained for a solution (1 mmol L<sup>-1</sup>) in CH<sub>2</sub>Cl<sub>2</sub> and *n*Bu<sub>4</sub>NPF<sub>6</sub> (0.3 mol L<sup>-1</sup>). Electro-syntheses of our films were performed with monomer solutions (1–2 mmol L<sup>-1</sup>) by continuous cycling between –0.2 and the appropriate potential (see Results and Discussion section) at *v* = 50 mV s<sup>-1</sup>. The films obtained were then copiously washed with fresh solvent before cycling. A platinum or gold electrode (0.07 cm<sup>2</sup>) was used as a working electrode for classical electrochemical characterisations. For in situ resistance experiments, gold and platinum six-band microelectrodes were designed on a glassy substrate by the microtechnologies department (DTA/LETI/DMITEC) of the CEA Grenoble. Interelectrode spacing was either 2 or 5 μm and the surface of each microelectrode was 0.66 mm<sup>2</sup>. Synthetic charge from 60 to 80 mC cm<sup>-2</sup> were typically necessary to electrically connect adjacent microelectrodes with the polymer. The stabilised power device used to connect the two outside electrodes was designed in our laboratories. The electrochemical and related resistance measurements were recorded with a BD91 Kipp&Zonen X-Y-Y' recorder that was previously kΩ calibrated with a RS components resistance box and the sample depth at the reduced state was measured using a Tencor profilometer. For demetallation experiments, cyanide solution was made from *n*Bu<sub>4</sub>NCN dissolved in CH<sub>3</sub>CN and lithium/cyanide solution from stoichiometric amounts of *n*Bu<sub>4</sub>NCN and LiClO<sub>4</sub> dissolved in CH<sub>3</sub>CN. The films were dipped for 20 min in one of these solutions and copiously washed with fresh CH<sub>3</sub>CN and then with CH<sub>2</sub>Cl<sub>2</sub> before cycling. Remetallations were performed by dipping films from 40 min to several hours in a copper(i) solution made from [Cu(CH<sub>3</sub>CN)<sub>4</sub>BF<sub>4</sub>] dissolved in CH<sub>3</sub>CN, followed by copious rinsing with fresh CH<sub>3</sub>CN and then CH<sub>2</sub>Cl<sub>2</sub>.

**2-(2-Thienyl)-1,10-phenanthroline:** 1,10-phenanthroline (4 g, 22.2 mmol) dissolved in toluene (50 mL) was cooled to 0 °C. The compound 2-thienyllithium (33 mL, 1 mol L<sup>-1</sup> in THF) was then added by the double-ended needle technique to this colourless solution. A dark red colour appeared immediately and after this the mixture was stirred at room temperature for 16 hours and cooled water saturated with NH<sub>4</sub>Cl was slowly added. After removal of organic solvents, CH<sub>2</sub>Cl<sub>2</sub> was added (100 mL) in several portions and the organic layer was separated. MnO<sub>2</sub> (50 g) was gradually added to this vigorously stirred dark brown solution over one hour until complete rearomatization had occurred (the reaction was monitored by thin layer chromatography). Addition of magnesium sulphate (50 g) and additional stirring (15 min) were followed by filtration on Celite and evaporation of the filtrate. This residue was purified by chromatography (silica gel, elution with CH<sub>2</sub>Cl<sub>2</sub>/1 % MeOH) to give 4.65 g of pure 2-(2-thienyl)-1,10-phenanthroline (80 %). <sup>1</sup>H NMR (200 MHz, CD<sub>2</sub>Cl<sub>2</sub>): δ = 9.20 (dd, *J* = 1.7 Hz, *J* = 4.35 Hz, 1H), 8.28 (dd, *J* = 1.7 Hz, *J* = 8.06 Hz, 1H), 8.26 (d, *J* = 8.35 Hz, 1H), 8.04 (d, *J* = 8.35 Hz, 1H), 7.84 (dd, *J* = 1.03 Hz, *J* = 3.8 Hz, 1H), 7.80 (d, 1H), 7.77 (d, 1H), 7.65 (dd, *J* = 8.06 Hz, *J* = 4.35 Hz, 1H), 7.53 (dd, *J* = 1.03 Hz, *J* = 5.1 Hz, 1H), 7.21 (dd, *J* = 5.1 Hz, *J* = 3.8 Hz, 1H); MS (FAB-MS): *m/z* (%): 262.3 (525 [2MH<sup>+</sup>], 263.1 [MH<sup>+</sup>], 179.2).

**2,9-Bis(2-thienyl)-1,10-phenanthroline (T<sub>1</sub>):** In a similar procedure, 2-thienyllithium (26 mL, 1 mol L<sup>-1</sup> in THF) was added to a solution of 2-(2-

thienyl)-1,10-phenanthroline (4.65 g, 17.8 mmol) in THF (50 mL). The solution immediately turned dark red and was stirred for 16 hours at room temperature. A work-up similar to the one described for 2-(2-thienyl)-1,10-phenanthroline was followed by chromatography (silica gel, CH<sub>2</sub>Cl<sub>2</sub>/1 % MeOH). The desired compound (918 mg) was isolated as an air- and light-stable yellow solid (50 %). <sup>1</sup>H NMR (200 MHz, CD<sub>2</sub>Cl<sub>2</sub>): δ = 8.21 (d, *J* = 8.4 Hz, 2H; H<sub>4</sub>), 7.99 (d, *J* = 8.4 Hz, 2H; H<sub>5</sub>), 7.86 (dd, *J* = 3.7 Hz, *J* = 1.0 Hz, 2H; H<sub>2</sub>), 7.71 (s, 2H; H<sub>3</sub>), 7.54 (dd, *J* = 5.0 Hz, *J* = 1.0 Hz, 2H; H<sub>2</sub>), 7.20 (dd, *J* = 3.7 Hz, *J* = 5.0 Hz, 2H; H<sub>6</sub>); MS (EI-MS): *m/z* (%): 344.4 (344.1 [M<sup>+</sup>]).

**2,9-Bis(2,2'-bithien-5-yl)-1,10-phenanthroline (T<sub>2</sub>):** The synthesis of this compound has already been reported<sup>[14, 16]</sup> and is similar to that of T<sub>1</sub> ligands (Scheme 2). C<sub>28</sub>H<sub>16</sub>N<sub>2</sub>S<sub>4</sub> (508.59): calcd C 66.11, H 3.17, N 5.51; found C 66.31, H 3.09, N 5.29.

**3,4-Dihexylthiophene:** [NiCl<sub>2</sub>(dppp)] (109 mg, 2 % mol) was added to 3,4-dibromothiophene<sup>[36]</sup> (2.4 g, 9.95 mmol) in THF (15 mL). *n*-Hexyl magnesium bromide (21.9 mmol, 2 mol L<sup>-1</sup> in ether) was slowly added to this vigorously stirred red mixture. The exothermicity was controlled with an ice bath. The resulting brown solution was then stirred at room temperature for 15 h and then cooled between 0 and 5 °C. Water that contained a few drops of HCl (1 mol L<sup>-1</sup>) was finally added. The solvents were removed and the organic material was extracted with CHCl<sub>3</sub> (60 mL). After the material was washed with brine (30 mL) and dried with MgSO<sub>4</sub>, the solvent was evaporated and the crude product was purified by chromatography (silica gel, hexane/1 % CHCl<sub>3</sub>) to give the desired compound as a colourless liquid (2.16 g, 86 %). <sup>1</sup>H NMR (200 MHz, CDCl<sub>3</sub>): δ = 6.89 (s, 2H), 2.50 (t, 4H), 1.65–1.30 (m, 16H), 0.89 (t, 6H); MS (FABMS): *m/z* (%): 252.5 (504 [2MH<sup>+</sup>], 253.2 [MH<sup>+</sup>], 181.1).

**2,5-Dibromo-3,4-dihexylthiophene:** *N*-bromosuccinimide (NBS) (730 mg, 4.1 mmol, previously recrystallised in acetic acid) was added in small portions to 3,4-dihexylthiophene (513 mg, 2 mmol) in acetic acid/CH<sub>2</sub>Cl<sub>2</sub> (1/1, 20 mL). The reaction was monitored by TLC and was completed within 2 h. H<sub>2</sub>O (10 mL) was slowly added to the mixture, followed by a saturated NaHCO<sub>3</sub> solution (50 mL) until the pH was neutral. After the organic solvent was removed, the product was washed with H<sub>2</sub>O/CH<sub>2</sub>Cl<sub>2</sub>. The organic layer was then dried with Na<sub>2</sub>SO<sub>4</sub> and concentrated. Chromatography (silica gel, hexane) gave a colourless liquid (710 mg, 86 %). <sup>1</sup>H NMR (200 MHz, CDCl<sub>3</sub>): δ = 2.52 (t, 4H), 1.58–1.20 (m, 16H), 0.89 (t, 6H); MS (FABMS): *m/z* (%): 410.3 (411 [MH<sup>+</sup>], 329.1).

**3',4'-Dihexyl-2,2':5',2''-terthiophene (DHTT):** The compound 2-bromothiophene (570 μL, 5.9 mmol) diluted in ether (10 mL) was slowly added to a solution of Mg (190 mg) in ether (5 mL) and a slight reflux was maintained. After 1 hour of reflux, this Grignard was transferred by means of the double-ended needle technique to a cold (–78 °C) mixture of 2,5-dibromo-3,4-dihexylthiophene (588 mg, 1.43 mmol) and [PdCl<sub>2</sub>(dppf)] (15 mg, 1 mol %) in ether (30 mL). The yellow mixture was then stirred at room temperature for 20 h. After cooling to between 0 and 5 °C, water that contained a few drops of HCl (1 mol L<sup>-1</sup>) was added to the mixture. After the organic solvents were removed, the product was washed with H<sub>2</sub>O/CH<sub>2</sub>Cl<sub>2</sub>. The organic layer was then dried with Na<sub>2</sub>SO<sub>4</sub> and concentrated. Chromatography (silica gel, hexane) gave a yellow pale liquid (535 mg, 90 %). <sup>1</sup>H NMR (200 MHz, CDCl<sub>3</sub>): δ = 7.32 (dd, *J* = 4.9 Hz, *J* = 1.2 Hz, 2H), 7.14 (dd, *J* = 3.7 Hz, *J* = 1.2 Hz, 2H), 7.07 (dd, *J* = 4.9 Hz, *J* = 3.7 Hz, 2H), 2.70 (t, 4H), 1.62–1.28 (m, 16H), 0.90 (t, 6H); MS (FABMS): *m/z* (%): 416.7 (416.4 [M<sup>+</sup>]).

**2-(3',4'-Dihexyl-2,2':5',2''-terthien-5-yl)-1,10-phenanthroline:** A solution of diisopropylamine (425 μL, 2.9 mmol) in THF (10 mL) was cooled to –78 °C. *n*-Butyllithium (1.7 mL, 1.77 mol L<sup>-1</sup> in hexane) was added dropwise to this solution. The mixture was stirred at –78 °C for 15 min, allowed to warm to 5 °C for 20 min and then cooled again to –78 °C before it was added by means of the double-ended needle technique to a cold (–78 °C) solution of DHTT (1.06 g, 2.55 mmol) in THF (25 mL). This mixture was stirred at –78 °C for 30 min and the temperature was increased to 0 °C before addition of the mixture to a colourless solution of 1,10-phenanthroline (328 mg, 1.82 mmol) in THF (10 mL) at room temperature. A dark red colour appeared immediately and this mixture was stirred at room temperature for 72 hours. Water saturated with NH<sub>4</sub>Cl was then slowly added. After removal of organic solvents, CH<sub>2</sub>Cl<sub>2</sub> (50 mL) was added and the organic layer was separated. MnO<sub>2</sub> (10 g) was progressively added to this vigorously stirred dark brown material until complete

rearomatisation occurred (the reaction was monitored by thin layer chromatography). Addition of magnesium sulphate (20 g) and additional stirring for 15 min was followed by filtration on Celite and evaporation of the filtrate. This residue was purified by chromatography (silica gel, progressive elution from hexane/10% CH<sub>2</sub>Cl<sub>2</sub> to CH<sub>2</sub>Cl<sub>2</sub>) to give pure 2-(3',4'-dihexyl-2,2':5',2''-terthien-5-yl)-1,10-phenanthroline (442 mg, 41%). <sup>1</sup>H NMR (200 MHz, CDCl<sub>3</sub>): δ = 9.23 (dd, 1H), 8.25 (d, 2H), 8.00 (d, 1H), 7.86 (d, 1H), 7.78 (s, 1H), 7.76 (s, 1H), 7.64 (dd, 1H), 7.33 (dd, 1H), 7.23 (d, 1H), 7.18 (dd, 1H), 7.09 (dd, 1H), 2.89–2.68 (m, 4H), 1.70–1.20 (m, 16H), 0.92 (t, 6H).

**2,9-Bis(3',4'-dihexyl-2,2':5',2''-terthien-5-yl)-1,10-phenanthroline (T<sub>3</sub>):** In a similar procedure, 5-lithio-3',4'-dihexyl-2,2':5',2''-terthiophene (1.1 mmol) in THF (10 mL) at 0 °C was added to a red orange solution of 2-(3',4'-dihexyl-2,2':5',2''-terthien-5-yl)-1,10-phenanthroline (442 mg, 0.75 mmol) in THF (30 mL). The solution immediately turned dark red and was stirred for 40 hours at room temperature. Hydrolysis, extraction with CH<sub>2</sub>Cl<sub>2</sub>, rearomatisation by MnO<sub>2</sub> (5 g) and then chromatography (silica gel, elution from hexane/10% CH<sub>2</sub>Cl<sub>2</sub> to CH<sub>2</sub>Cl<sub>2</sub>) afforded the desired compound (130 mg) isolated as an air- and light-stable red dark solid (34% yield, for a conversion of 58%). <sup>1</sup>H NMR (400 MHz, CD<sub>2</sub>Cl<sub>2</sub>): δ = 8.24 (d, 2H; H<sub>4</sub>), 7.99 (d, 2H; H<sub>3</sub>), 7.92 (d, 2H; H<sub>c</sub>), 7.74 (s, 2H; H<sub>5</sub>), 7.33 (dd, 2H; H<sub>a</sub>), 7.26 (d, 2H; H<sub>b</sub>), 7.17 (dd, 2H; H<sub>e</sub>), 7.08 (dd, 2H; H<sub>b</sub>), 2.88–2.65 (m, 8H; CH<sub>2ar</sub>, CH<sub>2ar</sub>), 1.7–1.2 (m, 32H), 0.98–0.82 (m, 12H; CH<sub>3</sub>); MS (FABMS): *m/z* (%): 1009.6 (1009.0 [M<sup>+</sup>], 925.0); C<sub>60</sub>H<sub>68</sub>N<sub>2</sub>S<sub>6</sub> (1009.08): C 71.38, H 6.79, N 2.27; found C 71.42, H 6.79, N 2.80.

**[Cu(T<sub>1</sub>)<sub>2</sub>BF<sub>4</sub>]:** [Cu(CH<sub>3</sub>CN)<sub>4</sub>BF<sub>4</sub>] (75 mg, 238 μmol) dissolved in CH<sub>3</sub>CN (25 mL) was added to a pale yellow solution of T<sub>1</sub> (150 mg, 436 μmol) in CH<sub>2</sub>Cl<sub>2</sub> (25 mL) by the double-ended needle transfer technique. The solution immediately turned red brown and was stirred for 40 min. The solvents were removed under vacuum and the product was dissolved in CH<sub>2</sub>Cl<sub>2</sub> and washed with H<sub>2</sub>O that contained a small amount of ascorbic acid. Filtration (silica gel, 5% MeOH/CH<sub>2</sub>Cl<sub>2</sub>) gave the desired product (180 mg, quantitative yield) as a dark red powder. <sup>1</sup>H NMR (CDCl<sub>3</sub>, 200 MHz): δ = 8.48 (d, 4H; H<sub>4</sub>), 8.02 (s, 4H; H<sub>3</sub>), 7.90 (d, 4H; H<sub>3</sub>), 7.21 (dd, 4H; H<sub>a</sub>), 6.77 (dd, 4H; H<sub>b</sub>), 6.34 (dd, 4H; H<sub>c</sub>).

**[Cu(T<sub>2</sub>)<sub>2</sub>BF<sub>4</sub>]:** A similar procedure gave this red orange complex (82%). <sup>1</sup>H NMR (400 MHz, CD<sub>2</sub>Cl<sub>2</sub>): δ = 8.37 (d, 4H; H<sub>4</sub>), 7.96 (d, 4H; H<sub>3</sub>), 7.85 (s, 4H; H<sub>5</sub>), 7.22 (d, 4H; H<sub>c</sub>), 7.11 (dd, 4H; H<sub>a</sub>), 6.79 (dd, 4H; H<sub>b</sub>), 6.59 (d, 4H; H<sub>b</sub>), 6.23 (dd, 4H; H<sub>c</sub>); MS (FABMS): *m/z* (%): 1080.9 (1081.0 [M – BF<sub>4</sub>]<sup>+</sup>, 571.0 [CuT<sub>2</sub><sup>+</sup>]); exact mass for C<sub>58</sub>H<sub>32</sub>N<sub>4</sub>S<sub>8</sub>Cu: calcd 1078.9689; found 1078.9708.

**[Cu(T<sub>3</sub>)<sub>2</sub>BF<sub>4</sub>]:** A similar procedure gave a dark red complex (95%). <sup>1</sup>H NMR (400 MHz, CD<sub>2</sub>Cl<sub>2</sub>): δ = 8.35 (d, 4H; H<sub>4</sub>), 7.94 (d, 4H; H<sub>3</sub>), 7.70 (s, 4H; H<sub>5</sub>), 7.42 (dd, 4H; H<sub>a</sub>), 7.30 (d, 4H; H<sub>c</sub>), 7.15 (dd, 4H; H<sub>b</sub>), 7.04 (dd, 4H; H<sub>c</sub>), 6.61 (d, 4H; H<sub>b</sub>), 2.54 (t, 8H; CH<sub>2ar</sub>), 2.12 (t, 8H; CH<sub>2ar</sub>), 1.55–0.70 (m, 88H); MS (FABMS): *m/z* (%): 2082.7 (2081.7 [M – BF<sub>4</sub>]<sup>+</sup>, 1997.1, 1071.0 [CuT<sub>3</sub><sup>+</sup>]); exact mass for C<sub>120</sub>H<sub>136</sub>N<sub>4</sub>S<sub>12</sub>Cu: calcd 2079.6710; found 2079.6848.

**XAS measurements:** XANES and EXAFS spectra were recorded at the European Synchrotron Research Facility [ESRF, Grenoble (France)] on the Collaborative Research Group IF-BM32 beamline equipped with a double-crystal monochromator of Si(111) and Si(311). The harmonics rejection was done with the use of a nickel-coated mirror first and a double platinum-coated mirror second. Energy resolution of the monochromator was Δ*E*/*E* = 2 × 10<sup>−4</sup>. All the samples have been studied at the Cu-K edge from 8875 to 9650 eV in fluorescence mode at room temperature. The K<sub>α</sub> fluorescence was measured with a Canberra detector that contained 27 elements, put perpendicularly into the incident beam to avoid scattered radiation. The X-ray absorption spectra were converted to an energy scale using copper foil as an internal standard with the energy of the maximum of the spectrum derivative of the copper foil's K edge defined as 8979 eV. The spectra of monomer model compounds have even been recorded and analysed.<sup>[16]</sup> The working electrode used for poly[Cu(T<sub>2</sub>)<sub>2</sub>] synthesis was a Toray Carbon Paper (not pretreated) purchased from E-TEK and it had a surface area measured at 0.27 mg cm<sup>−2</sup>. The conditions for the electropolymerisation were the same as described above, except for a scan rate of 10 mV s<sup>−1</sup> and a synthetic charge of 36 mC cm<sup>−2</sup>. For poly[Cu(T<sub>3</sub>)<sub>2</sub>], it was impossible to obtain a deposit thick enough with this working electrode and thus we used ELAT Solid Polymer Electrolyte electrodes loaded with platinum (5 mg cm<sup>−2</sup>) purchased from E-TEK. At the end of electro-

polymerisation, both samples were polarised for a few minutes at 0.0 V and then copiously rinsed with fresh solvent and stored under argon before use. The position of the samples was approximately 45° from the incident beam to maximise fluorescence detection. For data analysis, the analysis was made in harmonic approximation with plane waves<sup>[37]</sup> using a procedure described by D. Aberdam<sup>[38]</sup> and we have extensively described this for other experiments with related poly(metallorotaxane)s.<sup>[16]</sup>

## Acknowledgements

J. Serose (CEA Grenoble) is gratefully acknowledged for his help in the in situ resistance experiments. We thank D. Aberdam (CNRS) for helpful discussions and the technical staff of the BM32 beamline at the ESRF are thanked for technical guidance. We are also grateful to the Commissariat à l'Énergie Atomique for a fellowship for P.L. Vidal.

- [1] S. J. Higgins, *Chem. Soc. Rev.* **1997**, *26*, 247, and references therein.
- [2] a) F. Bedioui, J. Devynck, C. Bied-Charreton, *Acc. Chem. Res.* **1995**, *28*, 30; b) A. Deronzier, J. C. Moutet, *Coord. Chem. Rev.* **1996**, *147*, 339.
- [3] See for example: H. K. Youssoufi, M. Hmyene, F. Garnier, D. Delabouglisse, *J. Chem. Soc. Chem. Commun.* **1993**, 1550.
- [4] a) G. Bidan, B. Divisia-Blohorn, M. Lapkowski, J. M. Kern, J. P. Sauvage, *J. Am. Chem. Soc.* **1992**, *114*, 5986; b) J. M. Kern, J. P. Sauvage, G. Bidan, M. Billon, B. Divisia-Blohorn, *Adv. Mater.* **1996**, *8*, 580.
- [5] For an exhaustive review on conducting polymers that contain transition metals, see R. P. Kingsborough, T. M. Swager, *Prog. Inorg. Chem.* **1999**, *48*, 123.
- [6] a) T. Yamamoto, Y. Yoneda, T. Maruyama, *J. Chem. Soc. Chem. Commun.* **1992**, 1992; b) T. Yamamoto, T. Maruyama, Z. Zhou, T. Ito, T. Fukuda, Y. Yoneda, F. Begum, T. Ikeda, S. Sasaki, H. Takezoe, A. Fukuda, K. Kubota, *J. Am. Chem. Soc.* **1994**, *116*, 4832.
- [7] H. Segawa, N. Nakayama, F. Wu, T. Shimidzu, *Synth. Met.* **1993**, *55–57*, 966.
- [8] M. O. Wolf, M. S. Wrighton, *Chem. Mater.* **1994**, *6*, 1526.
- [9] G. Zotti, S. Zecchin, G. Schiavon, A. Berlin, G. Pagani, A. Canavesi, *Chem. Mater.* **1995**, *7*, 2309.
- [10] S. S. Zhu, T. M. Swager, *Adv. Mater.* **1996**, *8*, 497.
- [11] P. G. Pickup, C. G. Cameron, *Chem. Commun.* **1997**, 303.
- [12] S. S. Zhu, T. M. Swager, *J. Am. Chem. Soc.* **1997**, *119*, 12568.
- [13] Z. Peng, A. R. Gharavi, L. Yu, *J. Am. Chem. Soc.* **1997**, *119*, 4622.
- [14] P. L. Vidal, M. Billon, B. Divisia-Blohorn, G. Bidan, J. M. Kern, J. P. Sauvage, *Chem. Commun.* **1998**, 629.
- [15] J. L. Reddinger, J. R. Reynolds, *Chem. Mater.* **1998**, *10*, 3; J. L. Reddinger, J. R. Reynolds, *Chem. Mater.* **1998**, *10*, 1236.
- [16] P. L. Vidal, B. Divisia-Blohorn, G. Bidan, J. M. Kern, J. P. Sauvage, J. L. Hazemann, *Inorg. Chem.* **1999**, *38*, 4203–4210.
- [17] J. P. Sauvage, *Acc. Chem. Res.* **1990**, *23*, 321.
- [18] G. Bidan, M. Billon, B. Divisia-Blohorn, B. Leroy, P. L. Vidal, J. M. Kern, J. P. Sauvage, *J. Chim. Phys.* **1998**, *95*, 1254.
- [19] For a theoretical description of EXAFS spectroscopy, see E. A. Stern in *X-ray Absorption Principles, Applications, Techniques of EXAFS, SEXAFS and XANES* (Eds.: D. C. Koningsberger, R. Prins), Wiley-Interscience, New York, **1988**.
- [20] C. O. Dietrich-Buchecker, P. A. Marnot, J. P. Sauvage, J. P. Kintzinger, P. Maltese, *Nouv. J. Chim.* **1984**, *8*, 573.
- [21] C. Wang, M. E. Benz, E. LeGoff, J. L. Schindler, J. Allbritton-Thomas, C. R. Kannewurf, M. G. Kanatzidis, *Chem. Mater.* **1994**, *6*, 401.
- [22] A. K. I. Gushurst, D. R. McMillin, C. O. Dietrich-Buchecker, J. P. Sauvage, *Inorg. Chem.* **1989**, *28*, 4070.
- [23] We have previously reported the electro-synthesis of polyT<sub>2</sub> in CH<sub>3</sub>CN/Et<sub>4</sub>NBF<sub>4</sub> (0.1 mol L<sup>−1</sup>) ([18]). However, the polymer obtained by polymerisation in CH<sub>2</sub>Cl<sub>2</sub>/Bu<sub>4</sub>NPF<sub>6</sub> (0.3 mol L<sup>−1</sup>) exhibits a very similar electrochemical response.
- [24] J. Roncali, *Chem. Rev.* **1992**, *92*, 711.
- [25] J. Guay, P. Kasai, A. Diaz, R. Wu, J. M. Tour, L. H. Dao, *Chem. Mater.* **1992**, *4*, 1097.

- [26] P. Bäuerle, U. Segelbacher, K. U. Gaudl, D. Huttenlocher, M. Mehring, *Angew. Chem.* **1993**, *105*, 125; *Angew. Chem. Int. Ed. Engl.* **1993**, *32*, 76.
- [27] G. Zotti, R. A. Marin, M. C. Gallazi, *Chem. Mater.* **1997**, *9*, 2945.
- [28] H. D. Abbruña, J. H. White, M. J. Albarelli, G. M. Bommarito, M. J. Bedzyk, M. McMillan, *J. Phys. Chem.* **1988**, *92*, 7045.
- [29] C. O. Dietrich-Buchecker, J. P. Sauvage, J. M. Kern, *J. Am. Chem. Soc.* **1989**, *111*, 7791.
- [30] M. Geoffroy, M. Wermeille, C. O. Dietrich-Buchecker, J. P. Sauvage, G. Bernardinelli, *Inorg. Chim. Acta* **1990**, *167*, 157.
- [31] M. T. Miller, P. K. Gantzel, T. B. Karpishin, *Inorg. Chem.* **1998**, *37*, 2285.
- [32] L. S. Kau, D. J. Spira-Solomon, J. E. Penner-Hahn, K. O. Hodgson, E. I. Solomon, *J. Am. Chem. Soc.* **1987**, *109*, 6433.
- [33] M. Billon, G. Bidan, B. Divisia-Blohorn, J. M. Kern, J. P. Sauvage, P. Parent, *J. Electroanal. Chem.* **1998**, *456*, 91.
- [34] C. O. Dietrich-Buchecker, J. P. Sauvage, J. M. Kern, *J. Am. Chem. Soc.* **1984**, *106*, 3043.
- [35] D. Ofer, R. M. Crooks, M. S. Wrighton, *J. Am. Chem. Soc.* **1990**, *112*, 7869, and references therein.
- [36] J. M. Tour, R. Wu, *Macromolecules* **1992**, *25*, 1901.
- [37] B. K. Teo in *EXAFS Spectroscopy; Techniques and Applications* (Eds.: B. K. Teo, D. C. Joy), Plenum, New York, **1981**.
- [38] D. Aberdam, *J. Synchrotron Rad.* **1998**, *5*, 1287.

Received: June 1, 1999 [F1828]